IRSTI 29.05.41; 29.05.45 https://doi.org/10.26577/ijmph.20251611

G. Eswara Rao[1,2], V. Ganesh[2], Y. Aditya[3,*], U.Y. Divya Prasanthi[4]

[1]Department of Mathematics, Sri G.C.S.R. College, Rajam-532127, India
[2]Department of Mathematics, GIET University, Gunupur-765002, India
[3]Department of Mathematics, GMR Institute of Technology, Rajam-532127, India
[4]Department of Statistics & Mathematics, College of Horticulture, Dr. Y.S.R. Horticultural University, Parvathipuram-535502, India
*e-mail: aditya.y@gmrit.edu.in; yaditya2@gmail.com
(Received 10 January 2024; revised 26 February 2025; accepted 1 March 2025)

Bianchi Type-II Renyi Holographic Dark Energy Model in Saez-Ballester Theory of Gravity

Abstract. In Saez-Ballester's (Physics Letters A: 113, 467, 1986) theory of gravitation, the paper presents the study of Bianchi type-II interacting Rényi holographic dark energy. We determine interacting dark energy models by considering a correlation between the metric potentials to solve the field equations of the model. This results in a dynamical deceleration parameter demonstrating a shift in the cosmic rate of acceleration from deceleration to acceleration, with a redshift z change that is compatible with observations. Despite assuming several values to parameters ω_{de} close to –1 at $z = 0$ and is in agreement with the most recent observations. Next, we discovered that the squared sound speed, v_s^2, is negative at the initial epoch and positive at the present epoch, implying instability against perturbations at the initial epoch and stable at the present era. The $\omega_{de} - \omega'_{de}$ plane is constructed to investigate the evolution of the models' EoS parameter turned out to be in the freezing zone. As should be the case in an expanding universe, the strong energy conditions of the models are violated. Statefinders (r, s) plane confirms that our model includes the Chaplygin gas, phantom and ΛCDM limit.
Keywords: LRS Bianchi type-II metric, Saez-Ballester theory, Rényi holographic dark energy, scalar-tensor theory, cosmology.

Introduction

Cosmological acceleration is taking place in our universe. It is believed this is due to dark energy (DE), an enigmatic energy source with very negative pressure. Various cosmological observations have verified the existence of this kind of energy [1]-[2]. But what exactly it is is still a mystery that requires solving. Studying the dynamics of various DE models is one way to tackle the DE issue; modifying Einstein-Hilbert's action of general relativity results in new theories of gravity is the other. Equation of state (EoS) parameters allows DE models to be differentiated from the cosmological constant $\omega_{de} = p_{de}/\rho_{de}$, where p_{de} is the pressure and ρ_{de} is the energy density of DE. Scalar field models are among the most famous DE models presented in the literature [3]-[6]. Research into the theories of Brans-Dicke (BD) [7] and Saez-Ballester (SB) [8] as well as the f(R) and f(R,T) theories [9]-[10] (where R is the curvature scalar and T is the trace of the energy-momentum tensor) is influential in explaining the DE models among the many alternative theories of gravity. One may find a comprehensive analysis of DE models and revised theories of gravity in the cited works [12]–[14].

The metric potentials are associated with a dimensionless scalar field in the SB scalar-tensor theory of gravity. The SB theory of gravitation is a scalar-tensor theory that extends general relativity by incorporating a scalar field in the gravitational framework. This theory has been explored in the context of various cosmological models, particularly those involving holographic DE (HDE). The SB theory introduces a non-minimal coupling between the scalar field and the geometry of space-time. This coupling allows for richer dynamics compared to standard general relativity. In HDE models, scalar fields often play a crucial role in driving the accelerated expansion of the universe and in

explaining the nature of DE. The SB framework provides a flexible tool to model these scalar fields. When combined with the SB framework, the theory can provide insights into how scalar fields interact with holographic bounds to influence the accelerated expansion. The SB framework can be tuned to align with the observations while still exploring beyond-standard cosmology scenarios. The SB theory of gravitation provides a versatile and robust theoretical framework to extend the scope of HDE models. By incorporating scalar fields with non-minimal coupling, it allows for a deeper exploration of cosmological phenomena, addresses observational challenges, and opens avenues for connecting holography with fundamental aspects of gravitational physics. Saez and Ballester [8] start with the Lagrangian $L = R - \omega\phi^n\left(\phi_{,\mu}\phi^{,\mu}\right)$, where R is the scalar curvature; n, an arbitrary exponent; and ω, a dimensionless coupling constant. The independent variation of the metric tensor $g_{\mu\nu}$ and scalar field ϕ leads, respectively, to the field equations

$$R_{ij} - \frac{1}{2}Rg_{ij} - w\phi^n\left(\phi_{,i}\phi_{,j} - \frac{1}{2}g_{ij}\phi_{,k}\phi^{,k}\right) = = -\frac{8\pi G}{c^4}T_{ij} \quad (1)$$

$$2\phi^n\phi^i_{;i} + n\phi^{n-1}\phi_{,k}\phi^{,k} = 0 \quad (2)$$

using the matter's stress-energy tensor denoted by T_{ij}, the gravitational constant denoted by G, a dimensionless constant denoted by w, and partial and covariant differentiation, respectively, denoted by commas and semicolons. Here is the energy-conservation equation:

$$T^{ij}_{;j} = 0. \quad (3)$$

There has been a lot of focus on the holographic principle recently because of its significance in quantum gravity [15]-[17], where the entropy of a system is defined as one that depends on the surface area around it rather than the volume. There is a theoretical connection between infrared (IR) and ultraviolet (UV) cutoffs, and the holographic principle sets a maximum for the universe's entropy in a cosmic setting. The total energy in an area of size L cannot be more than the mass of a black hole of the same size if there is an energy density ρ_{de} in the UV-associated region, hence [5, 6]

$$L^3\rho_{de} \leq LM_p^2. \quad (4)$$

Here, the holographic energy density (HDE) is derived by taking into account the equality in Eq. (4), which allows us to find the maximum value of L

$$\rho_{de} = 3\xi^2 M_p^2 L^{-2}. \quad (5)$$

Here ξ is a numerical constant and $M_p^{-2} = 8\pi G$ is the reduced Planck mass. The future event horizon is the most accurate model for non-interacting HDE with an appropriate constant c, according to Li [6], whereas the Hubble and particle horizons do not fit well with the universe. Aviles et al. [18] have explored a model that explains cosmic acceleration and the role of dark matter within Einstein's theory of cosmology. The holographic energy density is sensitive to changes in the area law of entropy, which determines the energy density of the HDE. Entropy formalisms such as Tsallis HDE (THDE) [19], Sharma-Mittal HDE (SMHDE) [20], and Rényi HDE model (RHDE) [21] have been used for designing HDE models in recent times. The Chern-Simons theory of gravity has been used to examine the SMHDE, THDE, and RHDE cosmological models within the framework of the DGP braneworld, a D-dimensional fractal universe [22]-[23]. The observational restrictions on the RHDE models have been studied by Aditya et al. [26], Prasanthi and Aditya [24]-[25], and Aditya and Aditya [24]. Along with three other parametrizations of the dark matter/DE interaction, Sharma and Dubey [27] tested RHDE in an isotropic flat universe with the Hubble horizon as the infrared cutoff. As an IR cut-off, Chunlen and Rangdee [28] examined the RHDE model with particles and future horizons. Santhi and Chinnappalanaidu [29] studied RHDE in Ruban's Universe, with Hubble Horizon handling the infrared cutoff.

The fact that the visible universe is nearly homogenous and isotropic is well recognized. Therefore, the Friedmann-Robertson-Walker (FRW) models have garnered significant interest in the field of cosmology. Nevertheless, the presence of a limited number of variations in different directions during the first phases of the universe's development prompts us to examine the Bianchi type (BT) models,

which exhibit both uniformity and anisotropy. BT models are the most basic representation of an anisotropic world, characterised by spatial homogeneity, anisotropy, and a flat geometry. BT-II, VIII, and IX belong to the classification of spatially homogeneous but anisotropic cosmological models based on the Lie algebra of their isometry groups. Each type represents a different symmetry structure and geometric complexity, offering distinct insights into the dynamics of the universe in General Relativity. BT-II is simpler and often used as a stepping stone to explore general anisotropic behaviour. It provides insights into specific cosmic conditions without the full complexity of types VIII and IX. BT-VIII and IX are more critical for understanding the deep theoretical aspects of cosmology, such as chaotic dynamics, singularity structure, and the implications of anisotropy in quantum gravity and early-universe cosmology. Thus, while BT-II is valuable for specific, manageable problems, BT-VIII and IX are pivotal in addressing fundamental questions about the universe's origin and behaviour in extreme regimes. It represents a simpler anisotropic space-time with one degree of freedom in the anisotropy. It is simpler to study due to reduced complexity compared to types VIII and IX. It provides a bridge between fully isotropic models (like FRW) and complex anisotropic models (like VIII and IX). In recent studies, several authors have examined BT models while considering various factors like dust, stiff fluid, cosmic strings, and the cosmological constant. The purpose of these investigations is to explore the significance of anisotropies in the universe [30]-[38]. When there was a significant scalar field in gravity, Aditya and Reddy [39] described the BT model. Daniel Raju et al. [40]–[42] have conducted numerous studies on anisotropic DE models with huge scalar fields. An anisotropic cosmic model with a scalar field in $f(R,T)$ gravity has been studied by Aditya [43].

This study explores the BT-II Rényi holographic dark energy model inside the Saez-Ballester scalar-tensor theory of gravity, driven by the previous debate. Here is the structure of the paper: Our representation of the interacting RHDE model is given by the solutions to the field equations that we derive in Section 2. Also included in this part are the models' varied physical features. Section 3 includes a comparative analysis of our model with observational data. In Section 4, we provide an overview of the findings and interpretations.

Metric and field equations

We examine the BT-II space-time that is spatially homogenous as

$$ds^2 = dt^2 - \alpha^2(t)(dx^2 + dz^2) - \\ -\beta^2(t)(dy + xdz)^2 \quad (6)$$

where $\alpha(t)$ and $\beta(t)$ are the scale factors. The average scale factor and spatial volume are

$$a(t) = (\alpha^2\beta)^{\frac{1}{3}} \quad (7)$$

$$V = \alpha^2\beta. \quad (8)$$

The average Hubble parameter and scalar expansion θ are

$$H = \frac{\dot{a}}{a} = \frac{1}{3}\left(\frac{2\dot{\alpha}}{\alpha} + \frac{\dot{\beta}}{\beta}\right) \quad (9)$$

$$\theta = 3H = \frac{2\dot{\alpha}}{\alpha} + \frac{\dot{\beta}}{\beta}. \quad (10)$$

The shear scalar and average anisotropy of the model are

$$\sigma^2 = \frac{1}{3}\left(\frac{\dot{\alpha}}{\alpha} - \frac{\dot{\beta}}{\beta}\right)^2 \quad (11)$$

$$A_m = \frac{1}{3}\sum_{i=1}^{3}\left(\frac{\Delta H_i}{H}\right)^2. \quad (12)$$

where $\Delta H_i = H_i - H, i = 1,2,3,$ and $H_1 = H_2 = \frac{\dot{\alpha}}{\alpha}, H_3 = \frac{\dot{\beta}}{\beta}$.

SB field equations are given by (we assume $8\pi G = c = 1$)

$$R_{ij} - \frac{1}{2}Rg_{ij} - w\phi^n\left(\phi_{,i}\phi_{,j} - \frac{1}{2}g_{ij}\phi_{,k}\phi^{,k}\right) = \\ = -(T_{ij} + \overline{T}_{ij}) \quad (13)$$

$$2\phi^n\phi^i_{;i} + n\phi^{n-1}\phi_{,k}\phi^{,k} = 0 \quad (14)$$

$$\left(T_{ij} + \overline{T}_{ij}\right)_{;j} = 0. \quad (15)$$

which is the result of field equations (13) and (14). T_{ij} and $\overline{T}_{ij}$ are energy-momentum tensors for

pressure-less matter and Renyi HDE, which are defined as

$$T_{ij} = \rho_m u_i u_j; \tag{16}$$

$$\overline{T}_{ij} = [1, -(\omega_{de} + \zeta), - \\ -(\omega_{de} + \zeta), -\omega_{de}]\rho_{de} \tag{17}$$

here p_{de} and ρ_{de} are the pressure and energy density of DE, respectively, and ρ_m is the energy density of matter. Here skewness parameter ζ is the deviation from ω_{de} along x and y axes.

The field equations (13) for the metric (6) produce the following equations when adopting co-moving coordinates:

$$\frac{2\dot{\alpha}\dot{\beta}}{\alpha\beta} + \frac{\dot{\alpha}^2}{\alpha^2} - \frac{1}{4}\frac{\beta^2}{\alpha^4} + \frac{w}{2}\phi^n\dot{\phi}^2 = \rho_{de} + \rho_m \tag{18}$$

$$\frac{\ddot{\beta}}{\beta} + \frac{\ddot{\alpha}}{\alpha} + \frac{\dot{\alpha}\dot{\beta}}{\alpha\beta} + \frac{1}{4}\frac{\beta^2}{\alpha^4} - \frac{w}{2}\phi^n\dot{\phi}^2 = \\ = -(\omega_{de} + \zeta)\rho_{de} \tag{19}$$

$$\frac{2\ddot{\alpha}}{\alpha} + \frac{\dot{\alpha}^2}{\alpha^2} - \frac{3}{4}\frac{\beta^2}{\alpha^4} - \frac{w}{2}\phi^n\dot{\phi}^2 = -\omega_{de}\rho_{de} \tag{20}$$

$$\ddot{\phi} + \dot{\phi}\left(2\frac{\dot{\alpha}}{\alpha} + \frac{\dot{\beta}}{\beta}\right) + \frac{n}{2}\frac{\dot{\phi}^2}{\phi} = 0 \tag{21}$$

and

$$\dot{\rho}_m + \left(2\frac{\dot{\alpha}}{\alpha} + \frac{\dot{\beta}}{\beta}\right)\rho_m + \dot{\rho}_{de} + \\ + \left(2\frac{\dot{\alpha}}{\alpha} + \frac{\dot{\beta}}{\beta}\right)(1 + \omega_{de})\rho_{de} + 2\zeta\rho_{de}\frac{\dot{\alpha}}{\alpha} = 0, \tag{22}$$

where an overhead dot denotes differentiation with respect to cosmic time t.

Observations like the cosmic microwave background anisotropies, baryon acoustic oscillations, and weak lensing are sensitive to the interaction between matter and DE. Including interaction in cosmological models allows a better fit to data and can lead to new testable predictions, such as standard ΛCDM behaviour. With this motivation, here, we presume that DE and matter interact with one another. As a result, the energy-conservation equation Eq. (22) can be written for matter and DE as

$$\dot{\rho}_m + 3H\rho_m = Q, \tag{23}$$

$$\dot{\rho}_{de} + 3H(1 + \omega_{de})\rho_{de} + 2\zeta\rho_{de}\frac{\dot{\alpha}}{\alpha} = -Q. \tag{24}$$

Here Q is assumed as follows

$$Q = 3bqH\rho_{de} \tag{25}$$

where Q is the matter-DE interaction term and is a coupling constant (Xu [44]; Sobhanbabu and Santhi [45]). Because the positive parameter b will result in negative ρ_m in the flat universe, the parameter b is assumed to be negative. Q can shift its sign from $Q < 0$ to $Q > 0$ as the universe's expansion changes from deceleration ($q > 0$) to acceleration ($q < 0$). For $Q < 0$, energy moves from matter to RHDE, whereas for $Q > 0$, energy flows from RHDE to matter.

The field equations (18)-(21) create a system of four differential equations with seven unknowns, namely, α, β, ρ_{de}, ρ_m, ω_{de}, ζ and ϕ. Consequently, to get a precise answer to the nonlinear equations, we must presuppose that the shear scalar (Eq. (11)) is proportional to the scalar expansion (Eq. (10)), which in turn leads to a relationship between the metric potentials as described in [46]

$$\alpha = \beta^k \tag{26}$$

where $k \neq 1$ is a constant that preserves space-time's anisotropy. Using Eq. (26) in Eqs. (19) and (20), we get

$$\beta^{2k}\dot{\beta} = \beta_0\, exp\left(\int \left(\frac{\zeta\rho_{de} + \beta^{2(1-2k)}}{k-1}\right)\frac{\beta}{\dot{\beta}}\, dt\right). \tag{27}$$

We make the assumptions [47]-[49] to get the model's explicit solution

$$\zeta = \left[\frac{\zeta_0(k-1)\dot{\beta}}{\beta} - \beta^{2(1-2k)}\right]\frac{1}{\rho_{de}} \tag{28}$$

where ζ_0 is an arbitrary constant. From Eqs. (27) and (28), we obtain the metric potentials as

$$\alpha = \left[(2k+1)\left(\frac{\beta_0}{\zeta_0}\exp(\zeta_0 t) + \beta_1\right)\right]^{\frac{k}{2k+1}}; \\ \beta = \left[(2k+1)\left(\frac{\beta_0}{\zeta_0}exp(\zeta_0 t) + \beta_1\right)\right]^{\frac{1}{2k+1}} \tag{29}$$

where β_0 and β_1 are integrating constants. Using Eq. (29) in Eq. (21), we obtain the scalar field as

$$\phi = \left[\frac{(n+2)\phi_0}{2\beta_1\zeta_0(2k+1)} log\left(\frac{\beta_0}{\zeta_0} + \beta_1 exp(-\zeta_0 t)\right)\right]^{\frac{2}{n+2}}. \quad (30)$$

Using Eq. (29) the metric (6) can, now, be written as

$$ds^2 = dt^2 - \\ -\left[(2k+1)\left(\frac{\beta_0}{\zeta_0}\exp(\zeta_0 t) + \beta_1\right)\right]^{\frac{k}{2k+1}} \times \\ \times(dx^2 + dz^2) - \left[(2k+1)\left(\frac{\beta_0}{\zeta_0} exp(\zeta_0 t) + \right.\right. \\ \left.\left. +\beta_1\right)\right]^{\frac{k}{2k+1}} (dy + xdz)^2. \quad (31)$$

The mean Hubble parameter (H) and scalar expansion θ can be obtained as

$$H = \frac{\theta}{3} = \frac{1}{3}\left(2\frac{\dot{\alpha}}{\alpha} + \frac{\dot{\beta}}{\beta}\right) = \frac{b_0 exp(\zeta_0 t)}{3\left(\frac{b_0}{\zeta_0} exp(\zeta_0 t) + b_1\right)}. \quad (32)$$

The shear scalar σ^2 and average anisotropy A_m of the model are obtained as

$$\sigma^2 = \frac{(k-1)^2 b_0^2 exp(2\zeta_0 t)}{3\left(\frac{b_0}{\zeta_0} exp(\zeta_0 t) + b_1\right)^2}, \quad (33)$$

$$A_m = \frac{3(2k^2+1)}{(2k+1)^2}. \quad (34)$$

It is observed that the average anisotropic parameter A_m is constant throughout the evolution of the universe hence the model remains anisotropic. Also, for $k = 1$ the model becomes isotropic and shear free.

Rényi holographic dark energy: Tsallis ($\mathcal{S}_\mathcal{T}$) and Rényi ($\mathcal{S}_\mathcal{R}$) entropies are important generalized entropy parameters, and the relationship between them is given by

$$\mathcal{S}_\mathcal{R} = \frac{1}{\delta}\ ln(1 + \delta\mathcal{S}_\mathcal{T}). \quad (35)$$

$\mathcal{S}_\mathcal{T} = \frac{\mathcal{A}}{4}$. Here $\mathcal{A} = 4\pi L^2$ and L is the IR cutoff, is the Bekenstein entropy. We can determine the RHDE density using the relation $\rho_{de} dV \propto T\ dS$ as

$$\rho_{de} = \frac{3d^2}{L^2}(1 + \pi\delta L^2)^{-1}. \quad (36)$$

Here we assume the RHDE model with the Hubble horizon cutoff $L = H^{-1}$. We find the Hubble cutoff by inserting it into Eq. (36) as

$$\rho_{de} = \frac{3d^2H^2}{1+\pi\delta H^{-2}}. \quad (37)$$

The fractional energy densities of matter (Ω_m) and DE (Ω_{de}) are given as

$$\Omega_m = \frac{\rho_m}{\rho_{cr}} = \frac{\rho_m}{3H^2} \quad \text{and} \\ \Omega_{de} = \frac{\rho_{de}}{\rho_{cr}} = \frac{d^2}{1+\pi\delta H^{-2}}, \quad (38)$$

ρ_{cr} is the critical energy density. The non-interactive and interacting RHDE models are studied in the following sections, and the physical importance of various cosmological parameters is discussed.

Differentiating Eq. (37) with respect to time, we obtain

$$\dot{\rho}_{de} = \rho_{de}\left(\frac{4\dot{H}}{H} - \frac{2H\dot{H}}{H^2+\pi\delta}\right). \quad (39)$$

In view of Eqs. (32) and (39), from Eq. (24), we obtain the EoS parameter of RHDE as

$$\omega_{de} = -1 + b\left(1 + \frac{\dot{H}}{H^2}\right) + \frac{2\dot{H}}{3(H^2+\pi\delta)} - \frac{4\dot{H}}{H^2} - \frac{2\zeta_0 k(k-1)}{(2k+1)^2 H\Omega_{de}} + \frac{2k\beta^{2(1-2k)}}{3H^2(2k+1)\Omega_{de}} \quad (40)$$

where

$$\dot{H} = \frac{-b_0^2\ \exp(2\zeta_0\ t)}{3\left(\frac{b_0}{\zeta_0}\exp(\zeta_0 t) + b_1\right)^2} + \frac{b_0\ \zeta_0\ exp(\zeta_0\ t)}{3\left(\frac{b_0}{\zeta_0} exp(\zeta_0 t) + b_1\right)}. \quad (41)$$

Here Hubble parameter $H(t)$ and fractional energy density of RHDE Ω_{de} are respectively given in Eqs. (32) and (38).

EoS parameter ω_{de}: For $\omega = \frac{1}{3}$, $\omega = 1$ and $\omega = 0$ (decelerating phases), it contains radiation, stiff fluid and matter-dominated (dust), respectively. It symbolizes the quintessence for $-1 < \omega < -1/3$, the cosmological constant for $\omega = -1$, and the phantom for $\omega < -1$. For various values of d, the behaviour of the EoS parameter in terms of redshift for our interacting RHDE model is shown in Fig. 1. At first, the model starts in the matter-dominated period, then it fluctuates in the quintessence epoch, and finally it gets close to the phantom dividing line ($\omega_{de} = -1$). Our resulting model's EoS parameter $(z, \omega_{de}) = (0, -0.71)$ at z=0 agrees well with recent data from Planck [50].

$\omega_{de} - \omega'_{de}$ plane: Here, the behaviour of $\omega_{de} - \omega'_{de}$ (where prime represents the derivative about '$ln(a(t))$' plane is presented. This plane was initially suggested to investigate the evolution of the quintessence DE (Caldwell and Linder [51]). This plane can be divided into two portions, which are referred to as freezing ($\omega_{de} < 0$, $\omega'_{de} < 0$) and thawing ($\omega_{de} < 0$, $\omega'_{de} > 0$). By taking the derivative of Eq. (40) about $ln(a(t))$, we obtain

$$\omega'_{de} = \frac{2\ddot{H}(H^2 + \pi\delta) - 4\dot{H}^2 H}{3H(H^2 + \pi\delta)^2} - \frac{4}{3}\left[\frac{\ddot{H}}{H^2} - \frac{2\dot{H}^2}{H^3}\right] + \frac{2\zeta_0 k(k-1)}{(2k+1)^2}\left[\frac{\dot{H}}{H^3\Omega_{de}} + \frac{\dot{\Omega}_{de}}{\Omega_{de}H^2}\right]$$

$$+ \frac{2}{3(2k+1)}\left[\frac{2(1-2k)\beta^{1-4k}\dot{\beta}H^2\Omega_{de} - \beta^{2(2-2k)}(2H\dot{H}\Omega_{de} + H^2\dot{\Omega}_{de})}{H^5\Omega_{de}^2}\right] \quad (42)$$

where

$$\ddot{H} = \frac{2b_0^3\ exp(3\zeta_0\ t)}{3\left(\frac{b_0}{\zeta_0}exp(\zeta_0 t) + b_1\right)^3} - \frac{b_0^2\ \zeta_0\ exp(2\zeta_0\ t)}{\left(\frac{b_0}{\zeta_0}exp(\zeta_0 t) + b_1\right)^2} + \frac{b_0\ \zeta_0^2\ exp(\zeta_0\ t)}{3\left(\frac{b_0}{\zeta_0}exp(\zeta_0 t) + b_1\right)} \quad (43)$$

and

$$\dot{\Omega}_{de} = \frac{2H\dot{H}\pi\delta d^2}{(H^2 + \pi d)^2}. \quad (44)$$

For various values, we displayed in Figure 2 the behaviour of the $\omega_{de} - \omega'_{de}$ plane in our interacting RHDE model. Starting in the thawing area, our non-interacting RHDE model now fluctuates in the freezing region. Contemporary cosmological evidence suggests that the ice zone reveals an earlier cosmic acceleration period compared to the melting region. Therefore, our model agrees well with facts and shows cosmic acceleration in the frozen zone.

Squared sound speed v_s^2: This parameter v_s^2 is used to investigate the model's stability. If $v_s^2 > 0$, we get a stable model; otherwise ($v_s^2 < 0$), one can get an unstable model. Here, v_s^2 has the following form:

$$v_s^2 = \frac{\dot{p}_{de}}{\dot{\rho}_{de}} = \omega_{de} + \dot{\omega}_{de}\frac{\rho_{de}}{\dot{\rho}_{de}} =$$

$$= -1 + b\left(1 + \frac{\dot{H}}{H^2}\right) + \frac{2\dot{H}}{3(H^2 + \pi\delta)} - \frac{4\dot{H}}{H^2} - \frac{2\zeta_0 k(k-1)}{(2k+1)^2 H\Omega_{de}} + \frac{2k\beta^{2(1-2k)}}{3H^2(2k+1)\Omega_{de}}$$

$$+\{\frac{2\ddot{H}(H^2 + \pi\delta) - 4\dot{H}^2 H}{3H(H^2 + \pi\delta)^2} - \frac{4}{3}\left[\frac{\ddot{H}}{H^2} - \frac{2\dot{H}^2}{H^3}\right] + \frac{2\zeta_0 k(k-1)}{(2k+1)^2}\left[\frac{\dot{H}}{H^3\Omega_{de}} + \frac{\dot{\Omega}_{de}}{\Omega_{de}H^2}\right]$$

$$+ \frac{2\beta^{1-4k}}{3(2k+1)}\left[\frac{2(1-2k)\dot{\beta}H^2\Omega_{de} - \beta^3(2H\dot{H}\Omega_{de} + H^2\dot{\Omega}_{de})}{H^5\Omega_{de}^2}\right]\} \times \left(\frac{4\dot{H}}{H} - \frac{2H\dot{H}}{H^2 + \pi\delta}\right)^{-1}$$

Fig. 3 exhibits the behaviour of v_s^2 versus redshift. We notice that v_s^2 is initially negative, implying that our model is unstable. Furthermore, as the universe evolves, $v_s^2 > 0$ demonstrates model is stable. Hence, our model is stable at the present epoch.

Energy conditions: Initiating the study of energy conditions, the Raychaudhuri equations are fundamental when thinking about the congruence of time-like and null geodesics. The energy requirements are used to demonstrate other general theorems about the behaviour of powerful gravitational fields. We often see the following energy scenarios:

• Dominant energy condition (DEC): $\rho_{de} \geq 0$, $\rho_{de} \pm p_{de} \geq 0$.

• Strong energy conditions (SEC) : $\rho_{de} + p_{de} \geq 0$, $\rho_{de} + 3p_{de} \geq 0$,

• Null energy conditions (NEC): $\rho_{de} + p_{de} \geq 0$,

• Weak energy conditions (WEC): $\rho_{de} \geq 0$, $\rho_{de} + p_{de} \geq 0$,

Figure 4 illustrates the energy conditions for our models of RHDE. It is evident that the NEC is being violated, and as a consequence, the model indicates a Big Rip scenario. It is also seen that the WEC meets the requirement $\rho_{de} \geq 0$. In addition, Fig. 4 shows that the DEC $\rho_{de} + p_{de}$ is not satisfied. Additionally, our models violate the SEC, which is appropriate. This tendency, which is caused by the universe's late-time acceleration, is consistent with modern observational data.

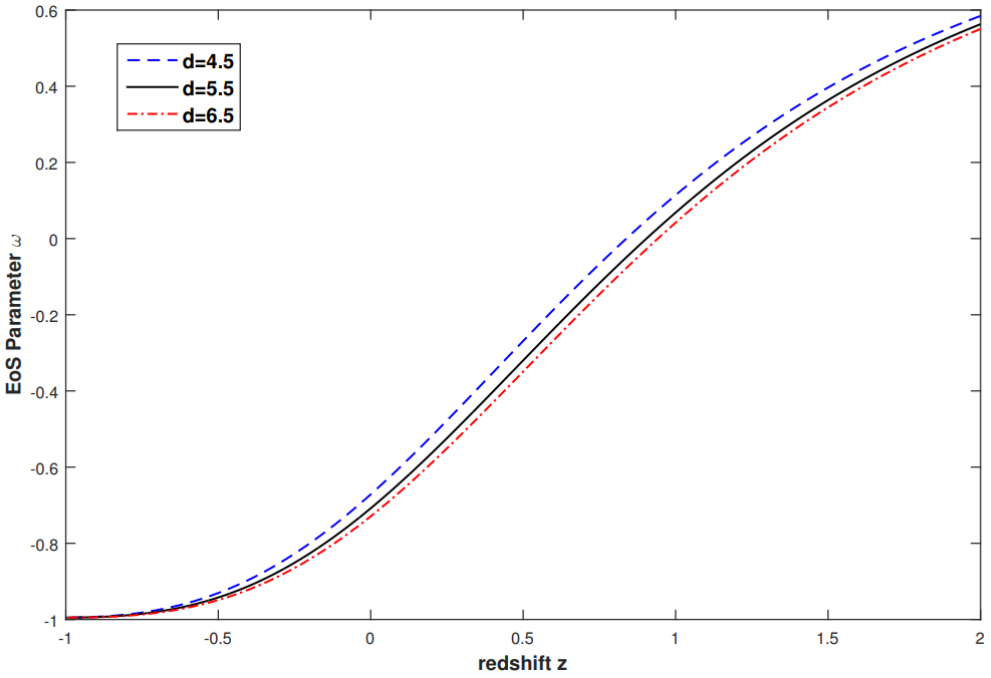

Figure 1 – Plot of EoS parameter ω_{de} versus redshift z for $\zeta_0 = 0.85$, $b_0 = 0.04$, $\delta = 0.00045$, $k = 0.98$, $b = 0.0045$ and $b_1 = -0.035$.

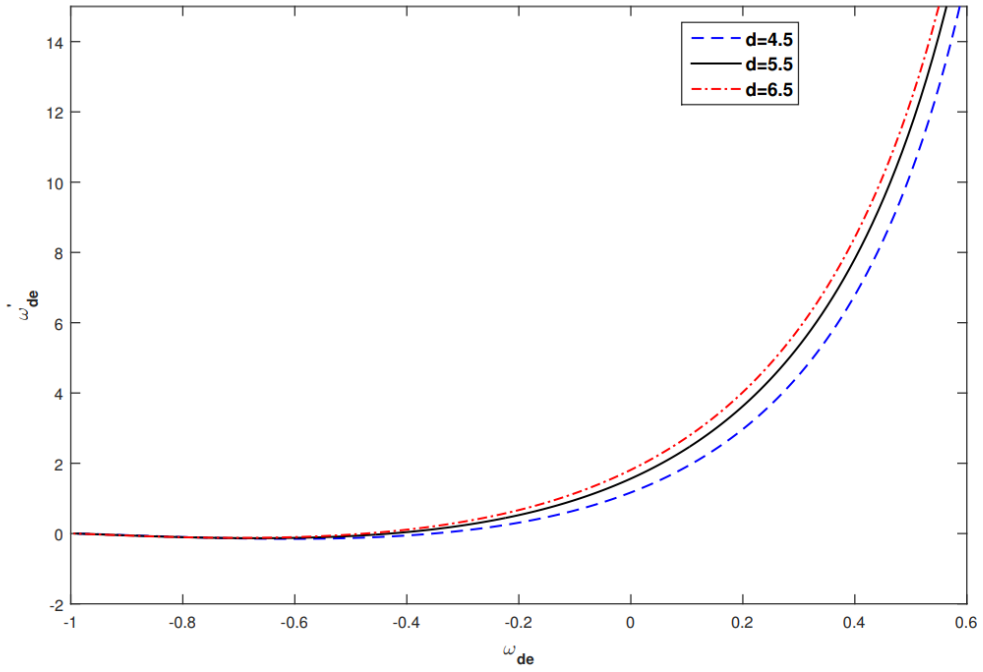

Figure 2 – Plot of $\omega_{de} - \omega'_{de}$ plane for $\zeta_0 = 0.85$, $b_0 = 0.04$, $\delta = 0.00045$, $k = 0.98$, $b = 0.0045$ and $b_1 = -0.035$.

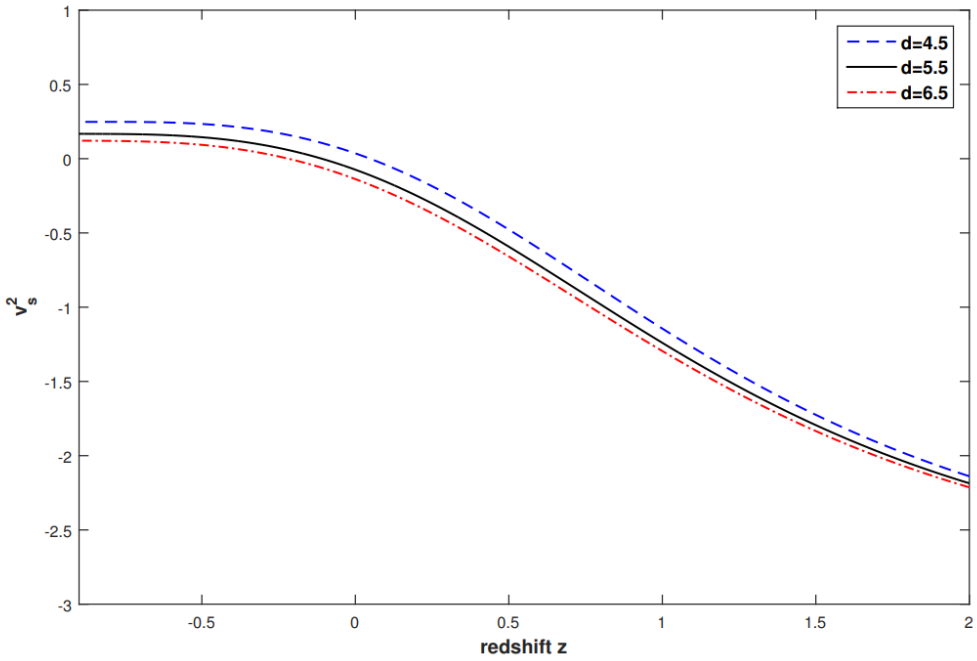

Figure 3 – Plot of v_s^2 versus redshift z for $\zeta_0 = 0.85$, $b_0 = 0.04$, $\delta = 0.00045$, $k = 0.98$, $b = 0.0045$ and $b_1 = -0.035$.

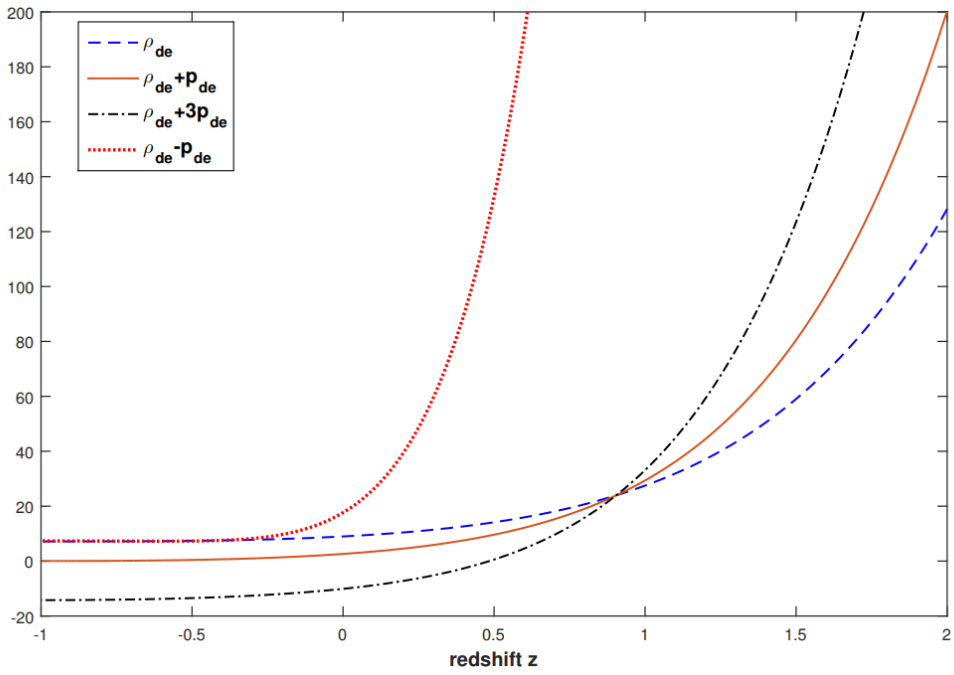

Figure 4 – Plot of energy conditions versus redshift z for $\zeta_0 = 0.85$, $b_0 = 0.04$, $\delta = 0.00045$, $k = 0.98$, $b = 0.0045$ and $b_1 = -0.035$.

Scalar field $\phi(t)$: For various values of b_1, Fig. 5 shows the behaviour of the ϕ(t) in terms of redshift, and Eq. (30) provides the scalar field of the models. Figure 5 shows that the scalar field is becoming smaller as the universe is getting older. Raju et al. [40, 41] found that the scalar field diminishes with cosmic duration in their analysis of the anisotropic DE and cosmic string cosmological model with a massive scalar field. Using a huge scalar meson field, Aditya et al. [52] addressed the BT-IX DE model in Lyra geometry. Rao et al. [53, 54] found a diminishing function of the scalar field in their study of the BT-I and BT-II massive scalar field models. Research into our scalar field is analogous to that of the DE models previously mentioned, as was established in the preceding debate. Further, it is observed that the scalar field representation is quite similar to exotic quasi-quintessence models widely investigated in the literature [55]-[58].

Deceleration parameter (DP): If the model accelerates or decelerates, it will be shown by the signature of the DP (q). When q>0, the model shows decelerating expansion; when q=0, it shows continuous expansion; and in the case where $-1 \leq q < 0$, it shows accelerating expansion. The cosmos displays super-exponential expansion for $q < -1$ and de Sitter (exponential) expansion for q=-1. For both the interacting and non-interacting cases, our model's DP is given by

$$q = -1 - \frac{\dot{H}}{H^2} = -1 - \frac{b_1\zeta_0}{b_0\ exp(\zeta_0\ t)}. \quad (45)$$

Figure 6 illustrates the relationship between the DP and the redshift z, considering various values of b_1. The model highlights the seamless transition from the universe's initial decelerated phase to its present accelerated phase. Around this region $0.65 < z < 0.85$, the universe changed from a decelerating to an accelerating phase. This is consistent with recent observations in cosmology [59, 60]. Capozziello et al. [59] examined the cosmographic constraints on the redshift at which the change from decelerating to accelerating expansion occurs in the f(R) theory of gravity. They found that the transition redshift (z_t) for the accelerating expansion lies between 0.3 and 0.8. In their study, Muthukrishna and Parkinson [60] examined the cosmographic assessment of the transition to acceleration by using SN-Ia and BAO. They determined the bounds on the transition redshift for different expansions and found that in the most conservative scenario, the change occurred at a redshift greater than 0.14 with a 95% confidence level.

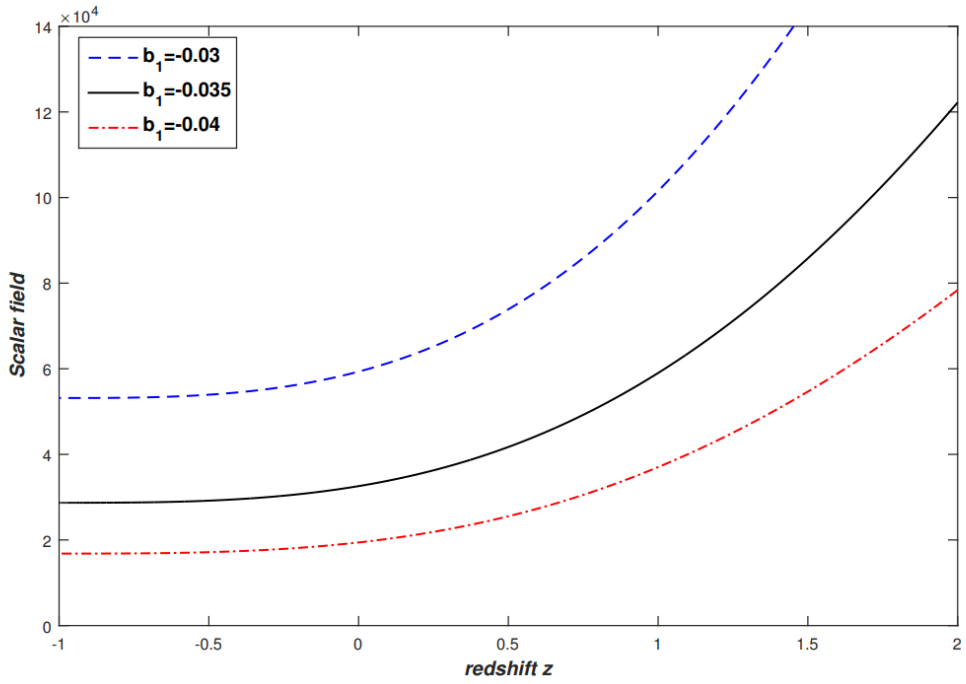

Figure 5- Plot of scalar field ϕ versus redshift z for $n = -1.5$, $\phi_0 = 1.5$, $\zeta_0 = 0.85$, $b_0 = 0.04$, $k = 0.98$ and $b_1 = -0.035$.

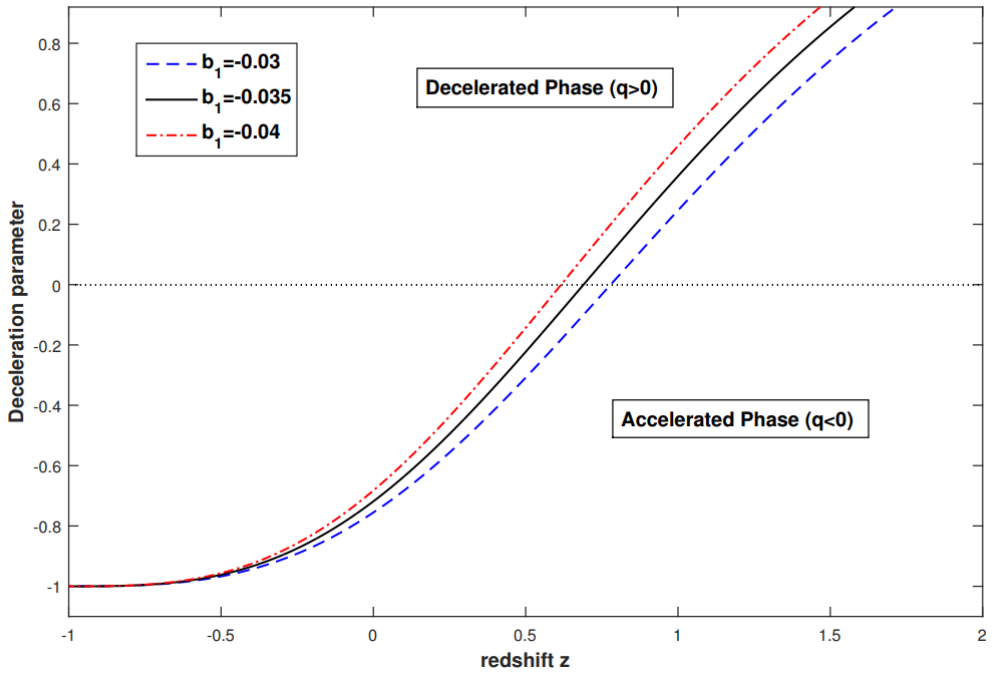

Figure 6 – Plot of DP q versus redshift z for $\zeta_0 = 0.85$ and $b_0 = 0.04$.

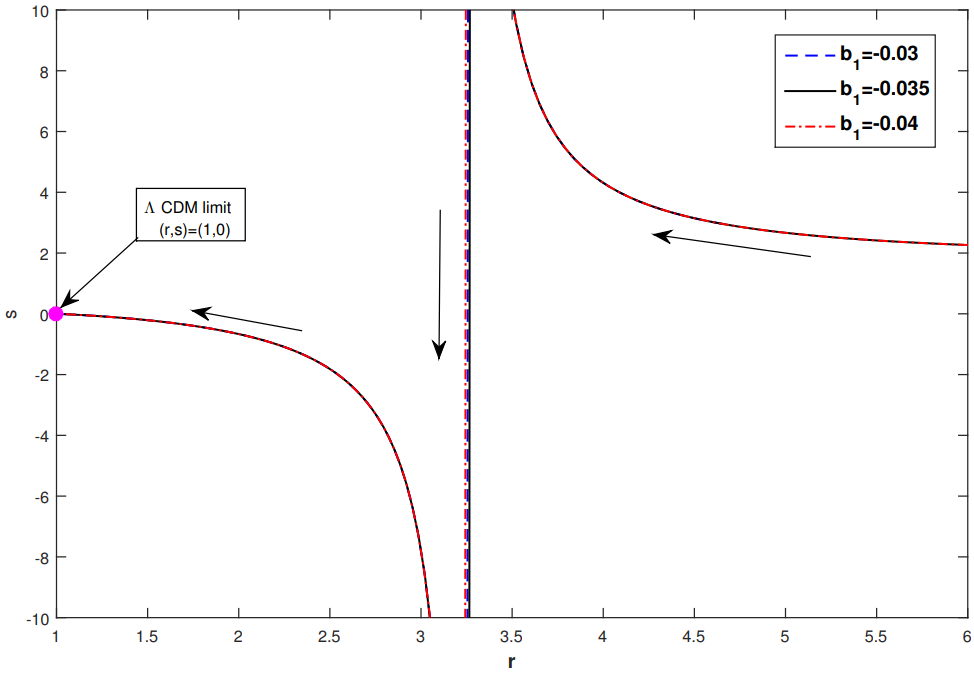

Figure 7 – Plot of $r-s$ plane for $\zeta_0 = 0.85$ and $b_0 = 0.04$.

Statefinder parameters: Several DE models have been proposed in recent years to elucidate the phenomenon of the universe's accelerating expansion. All of these different dark energy models have identical current values for their Hubble and DPs, which means they cannot be differentiated from one another. To do this, Sahni et al. [61] merged the deceleration and Hubble parameters, expressed as

$$r = \frac{\dddot{a}}{aH^3}, \quad s = \frac{r-1}{3(q-1/2)} \tag{46}$$

The regions shown below are defined by these statefinders: ΛCDM for $(r,s) = (1,0)$ and CDM model for $(r,s) = (1,1)$; $r < 1$ gives quintessence and $s > 0$ gives phantom DE phases; $r > 1$ with $s < 0$ establishes the Chaplygin gas model.

The statefinder parameters for our models are

$$r = 10 - \frac{18\zeta_0}{b_0\, exp(\zeta_0 t)}\left(\frac{b_0}{\zeta_0} exp(\zeta_0 t) + b_1\right) + \frac{9\zeta_0^2}{b_0^2\, exp(2\zeta_0 t)}\left(\frac{b_0}{\zeta_0} exp(\zeta_0 t) + b_1\right)^2 \tag{47}$$

$$s = \left[3 - \frac{6\zeta_0}{b_0\, exp(\zeta_0 t)}\left(\frac{b_0}{\zeta_0} exp(\zeta_0 t) + b_1\right) + \frac{3\zeta_0^2}{b_0^2\, exp(2\zeta_0 t)}\left(\frac{b_0}{\zeta_0} exp(\zeta_0 t) + b_1\right)^2\right] \times \left(-\frac{3}{2} - \frac{b_1\zeta_0}{b_0\, exp(\zeta_0\, t)}\right) \tag{48}$$

Figure 7 depicts the $r-s$ plane's trajectory. The $r-s$ plane resembles the ΛCDM model at late times. It can be seen that the behaviour of the $r-s$ plane is similar to that of dynamical DE models such as Chaplygin gas ($s<0$ and $r>1$) and phantom behaviour ($s>0$).

Results and Comparison

We compare our work to recent research on the topic and discuss how it matches up with observational data in this section.

Quintom and quasi-quintessence models aim to explain cosmic acceleration and dark energy, they approach the problem from very different perspectives. Quintom model through scalar fields and phantom energy crossing, and our model through holography, non-minimal coupling, and anisotropic space-time. Quintom model is primarily focused on dark energy driven by scalar fields and their equation of state, particularly with the possibility of crossing the phantom divide, allowing for a transition between decelerating and accelerating phases of the universe. The quasi-quintessence model is primarily concerned with the evolution of a scalar field whose equation of state evolves dynamically but stays above −1 providing a model for dark energy that does not cross the phantom divide. Our model combines anisotropic cosmologies, non-minimal coupling between scalar fields and curvature, and RHDE. This model is a more general and exotic approach to explaining dark energy. Thus, the main difference lies in the complexity of the framework and the inclusion of anisotropy and holographic principles in our model. However, it is very clear that our model completely varies in quintessence region and finally approaches the ΛCDM model.

Sadri and Vakili [62] investigated the FRW New HDE model in BD theory of gravity. They derived an EoS parameter that can enter the phantom regime ($\omega_{de} < -1$) without requiring interaction between DE and dark matter. Meanwhile, Sharif et al. [63] explored both interacting and non-interacting BT-I New HDE models in BD scalar-tensor gravity, obtaining a negative EoS parameter that results in an accelerating universe. Koussour et al. [64] examined the thermodynamic properties of a BT-I universe within a quadratic form of f(Q) gravity and discussed observational constraints. Their findings indicate that the EoS parameter ω_{de} is currently in the quintessence region and is projected to become less than -1 in the future. Furthermore, the present values of the EoS parameter, specifically ω_{de} = -0.92 for the Hubble dataset and ω_{de} = -0.794 for the combined Hz + SNe + BAO dataset, align well with recent observations from the Planck mission. Aditya [65] examined the Renyi HDE model within BT-I space-time under the SB theory of gravitation. The EoS parameter for this model is found to be close to -1 at z = 0, aligning with the latest observational data. Devi et al. [66] investigated the behaviour of Barrow HDE in the context of f(R, T) gravity against a flat FLRW space-time. They reported EoS parameter values of $-0.873^{+0.078}_{-0.115}$ and $-0.866^{+0.156}_{-0.130}$. Motaghi et al. [67] explored modified Barrow entropy about the cosmological background, employing the Friedmann equations. Their findings indicate that the EoS parameter resides in the quintessence region in the past and crosses the phantom divide in the present epoch. Chokyi et al. [68] discussed the Barrow HDE model within the SB framework in a homogeneous and anisotropic Kantowski-Sachs universe, analyzing both non-interacting and interacting scenarios, with the future event horizon acting as the infrared cut-off. Their study focused on the evolution of the EoS parameter for both situations. Sireesha nd Satyanarayana [69] discussed non-interacting RHDE models in the SB theory of gravity. Sobhanbabu et al. [70] investigated the BT-III HDE model within the SB scalar-tensor theory of gravitation, concluding that the EoS parameter varies significantly within the aggressive phantom region, which is consistent with modern Planck observational data. Luongo and Muccino [71] have revised the dynamics of the universe using high-redshift data from gamma-ray bursts to constrain cosmographic parameters. Luongo and Muccino [72] have addressed the circularity problem by using gamma-ray bursts as distance indicators through a new technique involving Bezier polynomials. Luongo and Muccino [73] investigated model-independent constraints on the universe's kinematics, focusing on snap-and-jerk terms. Carloni et al. [74] have investigated the impact of the dark energy spectroscopic instrument 2024 data on dark energy models.

ω_{de} value	Cosmological data sets
$-1.56^{+0.60}_{-0.48}$	$Planck + TT + lowE$
$-1.58^{+0.52}_{-0.41}$	$Planck + TT, TE, EE + lowE$
$-1.57^{+0.50}_{-0.40}$	$Planck + TT, TE, EE + lowE + lensing$
$-1.04^{+0.10}_{-0.10}$	$Planck + TT, TE, EE + lowE + lensing + BAO$

In our RHDE model, the analysis of the EoS parameter demonstrates that the model begins in a matter-dominated era, transitions through a quintessence phase, and ultimately approaches the phantom divide line (ω_{de} = -1). This behaviour is often referred to as having a ΛCDM nature. The present values of the EoS parameter for our model, at $z = 0$, are given by (d, ω_{de}) = (4.5, -0.68), (5.5, -0.72), (6.5, -0.78). These findings stand in contrast to the models discussed previously. Additionally, it is important to present the Planck observational data as reported by Aghanim et al. [50].

Final Remarks

This study explores the accelerating growth of the LRS BT-II universe by using the SB theory of gravity [8] and assuming the existence of RHDE. By utilizing the correlation between the metric potentials, we have derived a solution to the SB field equations, resulting in a variable DP. We examined many cosmological parameters to evaluate the accuracy of these findings. The results of our investigation are as follows:

- The scalar field ϕ decreases as the universe evolves. According to the literature (Raju et al. [41, 42]; Aditya et al. [52]; Rao et al. [53, 54]), the study of our scalar field is very similar to the previously mentioned dark energy models. The NEC is violated, and hence the model results in a Big Rip (Fig. 4). The WEC satisfied $\rho_{de} \geq 0$, however, the DEC $\rho_{de} + p_{de}$ did not satisfy. Additionally, as should be the case, our model violates the SEC. This tendency, which is caused by the universe's late-time acceleration, is consistent with recent observational data.
- Examination of the EoS parameters reveals that the anisotropic RHDE model starts in the matter-dominated zone, crosses the quintessence region and approaches to phantom dividing line i.e., ΛCDM model. Furthermore, it is useful to show here that the current values of the EoS parameter value in our model $\omega_{de} \approx -0.78$ is in good agreement with Planck's observed data (Aghanim et al. [50]). It demonstrates the agreement of our findings with the cosmic observations.
- The $\omega_{de} - \omega'_{de}$ plane for our RHDE models is shown in Fig. 2, and the trajectories meet both freezing and thawing zones. However, in the present and future, the models only show freezing regions. Recent observations confirm that models that differ in the freezing area are the best candidates for explaining cosmic acceleration. The stability analysis shows that the models (ref. Fig. 3) are unstable in the past but stable in the present and future eras.
- The DP experiences a change in its signature, changing from positive to negative or vice versa. The model illustrates the smooth shift from the initial decelerated phase to the current accelerated phase of the cosmos. The transition redshift of the universe (Fig. 6) at $0.65 < z < 0.85$. At a 95% confidence level, this is in agreement with SN-Ia and BAO cosmological observations [59, 60]. Furthermore, the current value of the DP $q(t)$ for our models is $q \approx -0.72$, which is consistent with the modern observations [75, 76] given as $q = -0.930 \pm 0.218$ $(BAO + Masers + TDSL + Pantheon + H_z)$.
- At late times, the statefinder plane $(r - s)$ corresponds to the ΛCDM model, and its behaviour is identical to that of the dynamical DE model, such as Chaplygin gas ($s < 0$ and $r > 1$) and phantom model ($s > 0$) (Fig. 7).

Acknowledgements. The authors are grateful to the anonymous reviewers for their constructive comments which have improved the presentation of the work. Y. Aditya is thankful to the National Board for Higher Mathematics, Department of Atomic Energy, Govt. of India for its financial support under grant No: 02011/8/2023 NBHM(R.P.)/R & D II/3073.

References

1. Riess, A. G. et al. “Observational evidence from supernovae for an accelerating universe and a cosmological constant”. *The Astronomical Journal*, 116(3) (1998): 1009, doi: 10.1086/300499

2. Perlmutter, S. et al. “Measurements of Ω and Λ from 42 High-Redshift Supernovae”, *The Astrophysical Journal,* 517 (1999): 565, doi: 10.1086/307221

3. Kamenshchik, A.Y., et al. “An alternative to quintessence” *Phys. Lett. B* 511 (2001) 265-268, doi: 10.48550/arXiv.gr-qc/0103004

4. Bento, M.C., et al. “Generalized Chaplygin gas, accelerated expansion, and dark-energy-matter unification” *Physical Review D*, 66 (2002) :043507, doi:10.1103/PhysRevD.66.043507

5. Hsu, S.D.H. “Entropy Bounds and Dark Energy” *Phys. Lett. B* 594 (2004) :13-16. Doi:10.48550arXivhep-th/0403052

6. Li, M. “A model of holographic dark energy.” *Physics Letters B*, *603*(1-2) (2004) :1-5, doi: 10.1016/j.physletb.2004.10.014.

7. Brans, C., Dicke, R.H. “Mach's Principle and a Relativistic Theory of Gravitation.” *Physical Review Journals*, 594 (1961) :13, doi:10.1103/PhysRev.124.925

8. Saez, D., Ballester, V. J. “A simple coupling with cosmological implications.” *Physics Letter A*, 113 (1986) :467. doi:10.1016/0375-9601(86)90121-0

9. Capozziello, S., Laurentis, M. De. “Extended Theories of Gravity.” *Physics Reports*, 509 (2011) :167-321. doi:10.1016/j.physrep.2011.09.003

10. Harko, T., et al., “f(R,T) gravity.” *Physical Review D*, 84 (2011) :024020. doi:10.1103/PhysRevD.84.024020

11. Copeland, E. J., et al. “Dynamics of dark energy.” *International Journal of Modern Physics D*, *15*(11) (2006) :1753-1935, doi: 10.1142/S021827180600942X

12. Clifton, T., et al., “Modified Gravity and Cosmology.” *Physics Reports*, 513 Phys. Rep. (2012) :1-189. doi: 10.1016/j.physrep.2012.01.001

13. Bamba, K., et al. “Dark energy cosmology: the equivalent description via different theoretical models and cosmography tests.” *Astrophysics and Space Science*, *342* (2012) :155-228. doi: 10.48550/arXiv.1205.3421.

14. Nojiri, S., et al. “Modified gravity theories on a nutshell: Inflation, bounce and late-time evolution.” *Physics Reports*, 692 (2017) :1-104, doi: 10.1016/j.physrep.2017.06.001.

15. Hooft. G. ’t. “Dimensional Reduction in Quantum Gravity.” (2009). doi: 10.48550/arXiv.gr-qc/9310026

16. Cohen, A. G., et al. “Effective field theory, black holes, and the cosmological constant.” *Physical Review Letters*, 82(25) (1999) :4971. doi: 10.1103/PhysRevLett.82.4971.

17. Susskind, L. “The world as a hologram.” *Journal of Mathematical Physics*, 36(11) (1995) :6377-6396. doi: 10.1063/1.531249

18. Aviles, A., et al. “Holographic dark matter and dark energy with second order invariants.” *Phys. Rev. D*, 84 (2011): 103520. https://doi.org/10.1103/PhysRevD.84.103520

19. Tavayef, M., et al. “Tsallis holographic dark energy.” *Phys. Lett. B.* 781 (2018) :195. doi:10.1016/j.physletb.2018.04.001

20. Jahromi, A. S., et al. “Generalized entropy formalism and a new holographic dark energy model.” *Physics Letters B*, 780 (2018) :21-24, doi: 10.1016/j.physletb.2018.02.052.

21. Moradpour, H., et al. “Thermodynamic approach to holographic dark energy and the Rényi entropy.” *The European Physical Journal C* 78 (2018) :829. https://doi.org/10.1140/epjc/s10052-018-6309-8

22. Maity, S., & Debnath, U. “Tsallis, Rényi and Sharma-Mittal holographic and new agegraphic dark energy models in D-dimensional fractal universe.” *The European Physical Journal Plus*, 134(10) (2019) :514, doi: 10.1140/epjp/i2019-12884-6.

23. Iqbal, A., & Jawad, A. “Tsallis, Renyi and Sharma–Mittal holographic dark energy models in DGP brane-world.” *Phys. Dark Univ*. 26, (2019) :100349, doi: 10.1016/j.dark.2019.100349.

24. Divya Prasanthi, U.Y., Aditya, Y. “Observational constraints on Renyi holographic dark energy in Kantowski–Sachs universe.” *Phys. Dark Univ*. 31 (2021) :100782 doi: 10.1016/j.dark.2021.100782

25. Divya Prasanthi, U.Y., Aditya, Y. “Anisotropic Renyi holographic dark energy models in general relativity.” *Results in Physics*, 17 (2021) :103101. doi: org/10.1016/j.rinp.2020.103101

26. Aditya, Y., Mandal, S., Sahoo, P. K., & Reddy, D. R. K. “Observational constraint on interacting Tsallis holographic dark energy in logarithmic Brans–Dicke theory.” *The European Physical Journal C*, 79(12) (2019) :1020. https://doi.org/10.1140/epjc/s10052-019-7534-5

27. Sharma, U.K., Dubey, V.Ch. “Phantom dark energy nature of bulk-viscosity universe in modified f(Q)-gravity.” *Int. J. Geom. Theories Mod. Phys.* 19(1) (2022) :2250010. doi:10.1142/S0219887822501985

28. Chunlen, S., Rangdee, P. “Exploring the Rényi Holographic Dark Energy Model with the Future and the Particle Horizons as the Infrared Cut-off.” *Phayao Research Conference* 10 (2021) :2413, doi:10.48550/arXiv.2008.13730

29. Santhi, M.V., Chinnappalanaidu, T. “Some Bianchi Type Viscous Holographic Dark Energy Cosmological Models in the Brans–Dicke Theory.” *New Astr.* 92 (2022) :101725. doi:10.1155/2022/5364541

30. Santhi M.V., Rao V.U.M., and Aditya Y. “Bulk viscous string cosmological models in f(R) gravity.” *Canadian Journal of Physics* 56 (2017) :362 doi: .org/10.1139/cjp-2017-0256.

31. Rao, V.U.M., Prasanthi, U.Y.D. “Bianchi type-I and -III modified holographic Ricci Dark energy models in Saez- Ballester theory.” *The European Physical Plus* 132 (2017) :64. doi:10.1140/epjp/i2017-11328-9

32. Santhi, M. V., Rao, V. U. M., & Aditya, Y. “Anisotropic magnetized holographic Ricci dark energy cosmological models.” *Canadian Journal of Physics*, *95*(4) (2017) :381-392. https://doi.org/10.1139/cjp-2016-0781

33. Mishra, B., et al. “Bianchi-V string cosmological model with dark energy anisotropy.” *Astrophys. Space Sci.* 363 (2018) : 86. https://doi.org/10.1007/s10509-018-3313-2

34.Aditya, Y., Reddy, D.R.K. "Dynamics of perfect fluid cosmological model in the presence of massive scalar field in $f(R,T)$ gravity." *Int. J. Geom. Theories Mod. Phys.* 15(9) (2018) : 1850156. DOI: 10.1007/s10509-018-3491-y

35.Naidu, R.L. "Bianchi type-II modified holographic Ricci dark energy cosmological model in the presence of massive scalar field." *Can J Phys.* 97(3) (2019) :330. doi: 10.1139/cjp-2017-0716

36.Naidu, R.L., et al. "Bianchi type-V dark energy cosmological model in general relativity in the presence of massive scalar field." *Heliyon* 5(5) (2019) :E01645. doi:10.1016 j.heliyon.2019.e01645

37.Reddy, D.R.K., Aditya, Y., & Naidu, K.D. "Dynamics of Bianchi type-II anisotropic dark energy cosmological model in the presence of scalar-meson fields." *Canadian Journal of Physics*, *97*(9) (2019) :932-937. doi: 10.1139/cjp-2018-0403.

38.Aditya, Y., Raju, K. D., Rao, V. U. M., & Reddy, D. R. K. "Kaluza-Klein dark energy model in Lyra manifold in the presence of massive scalar field." *Astrophysics and Space Science*, 364 (2019) :190. https://doi.org/10.1007/s10509-019-3681-2

39.Aditya, Y., Reddy, D. R. K. "Dynamics of perfect fluid cosmological model in the presence of massive scalar field in f(R,T) gravity" *Astrophysics and Space Science*, 364 (2019) : 3. https://doi.org/10.1007/s10509-018-3491-y.

40.Raju, K. D., et al. "Bianchi type-III dark energy cosmological model with massive scalar meson field" *Astrophysics and Space Science*, *365* (2020) :45. https://doi.org/10.1007/s10509-020-03753-1

41.Raju, K. D., et al. "Kantowski–Sachs universe with dark energy fluid and massive scalar field." *Canadian Journal of Physics* 98 (2020) :993. https://doi.org/10.1139/cjp-2019-0563

42.Raju, K. D., et al. "Bianchi type-V string cosmological model with a massive scalar field" *Astrophysics and Space Science*, *365*, (2020) :28. https://doi.org/10.1007/s10509-020-3729-3

43.Aditya, Y. "Anisotropic cosmological model with a massive scalar field in f (R, T) gravity." *Bulgarian Astronomical Journal*, *39* (2023) :12. https://www.astro.bas.bg/AIJ/issues/n39/YAditya.pdf

44.Xu, Y.D. "Tsallis agegraphic dark energy model with the sign-changeable interaction." *Commun. Theor. Phys* 72 (2020) :015402. doi: 10.1088/1572-9494/ab544e

45.Sobhanbabu, Y., Santhi, M.V. "Kantowski-Sachs Tsallis holographic dark energy model with sign-changeable interaction." *Eur. Phys. J. C* 81 (2021) :1040. https://doi.org/10.1140/epjc/s10052-021-09815-0

46.Collins, C. B., Glass, E. N., & Wilkinson, D. A. "Exact spatially homogeneous cosmologies." *General Relativity and Gravitation*, 12 (1980) :805-823. doi: 10.1007/BF00763057.

47.Adhav. K.S. "LRS Bianchi Type-I Universe with Anisotropic Dark Energy in Lyra Geometry." *Astron. Astrophys*, 1(4) (2011) :204. doi: 10.4236/ijaa.2011.14026

48.Santhi, M. V., Aditya, Y., & Rao, V. U. M. "Some Bianchi type generalized ghost piligrim dark energy models in general relativity." *Astrophysics and Space Science*, 361(4) (2016) :142. https://doi.org/10.1007/s10509-016-2731-2

49.Aditya, Y., & Reddy, D. R. K. "Anisotropic new holographic dark energy model in Saez–Ballester theory of gravitation." *Astrophysics and Space Science*, 363(10) (2018) :207. DOI: 10.1007/s10509-018-3429-4

50.Aghanim, N., et al. "Planck 2018 results. [Plancks Collaboration]" *A&A* 641 (2020) :A6. doi:10.1051/0004-6361/201833910

51.Caldwell, R. R., & Linder, E. V. "Limits of quintessence." *Physical review letters*, 95(14) (2005) :141301. doi: 10.1103/PhysRevLett.95.141301.

52.Aditya, Y., Divya Prasanthi, U. Y., & Reddy, D. R. K. Bianchi type-IX model in the presence of anisotropic dark energy and massive scalar meson field in Lyra geometry. *International Journal of Modern Physics A*, 37(16) (2022) :2250107, doi: 10.1142/S0217751X2250107X

53.Bhaskara Rao, M.P.V.V., et al. "Anisotropic cosmological model with a massive scalar field in f (R, T) gravity." *New Astr* 92 (2022) :101733. DOI:10.1016/j.newast.2021.101733

54.Bhaskara Rao, M.P.V.V., et al. "Anisotropic minimally interacting dark energy models with cosmic strings and a massive scalar field." *International Journal of Modern Physics* A 36(36) (2021) :2150260. doi:10.1142/S0217751X21502602

55.Luongo, O., & Muccino, M. "Speeding up the universe using dust with pressure." *Phys. Rev. D* 98 (2018): 103520. https://doi.org/10.1103/PhysRevD.98.103520

56.D'Agostino, R., Luongo, O., & Muccino, M. "Healing the cosmological constant problem during inflation through a unified quasi-quintessence matter field." Class. Quant. Grav., 39 (2022): 195014. https://doi.org/10.1088/1361-6382/ac8af2

57. Luongo, O., & Mengoni, T. "Quasi-quintessence inflation with non-minimal coupling to curvature in the Jordan and Einstein frames." arXiv:2309.03065 (2023).

58.Belfiglio, A., Giambò, R., & Luongo, O. "Alleviating the cosmological constant problem from particle production." *Class. Quant. Grav*. 40(10) (2023): 105004. https://doi.org/10.1088/1361-6382/accc00

59.Capozziello, S., Farooq, O., Luongo, O., & Ratra, B. "Cosmographic bounds on the cosmological deceleration-acceleration transition redshift in f (R) gravity." *Physical Review D*, 90(4) (2014) :044016, doi: 10.1103/PhysRevD.90.044016.

60.Muthukrishna, D., & Parkinson, D. "A cosmographic analysis of the transition to acceleration using SN-Ia and BAO." *Journal of Cosmology and Astroparticle Physics*, 2016(11) (2016) :052, doi: 10.1088/1475-7516/2016/11/052.

61.Sahni, V., Saini, T. D., Starobinsky, A. A., & Alam, U. "Statefinder—a new geometrical diagnostic of dark energy." *Journal of Experimental and Theoretical Physics Letters*, 77 (2003) :201-206. https://doi.org/10.1134/1.1574831.

62.Sadri, E., Vakili, B. "Exploring cosmological models in modified gravity theories." *Astrophys. Space Sci.* 363 (2018): 13. doi:10.1007/s10509-017-3232-0.

63.Sharif, M., et al. "Impact of modified gravity theories on symmetry and stability." *Symmetry* 10 (2018): 153. doi:10.3390/sym10050153.

64.Koussour, M., et al. "Holographic dark energy models in anisotropic spacetimes." *Journal of High Energy Astrophysics* 37 (2023): 15. doi:10.1016/j.jheap.2023.05.002.

65.Aditya, Y. "Dynamics of anisotropic Renyi holographic dark energy model" *Bulgarian Astronomical Journal* 40 (2024): 95.

66.Devi, K., et al. “Holographic dark energy in Barrow cosmology with Granda-Oliveros IR cutoff” *Astrophys. Space Sci.* 369 (2024): 73. doi:10.1007/s10509-023-04122-y.

67.Motaghi, M., et al. “Holographic dark energy in Barrow cosmology with Granda-Oliveros IR cutoff.” *arXiv preprint*, arXiv:2407.21074 (2024). doi:10.48550/arXiv.2407.21074.

68.Chokyi, K. K., et al. “Investigating energy conditions in holographic dark energy.” *Phys. Scr.* 99 (2024): 111501. doi:10.1088/1402-4896/acf202.

69.Sireesha, K.V.S., Satyanarayana, P., “Renyi Holographic dark energy models in SaezBallester theory of gravitation”. DOI: https://doi.org/10.21203/rs.3.rs-3969986/v1 (2024).

70.Sobhanbabu, Y., et al. “Anisotropic Barrow Holographic Dark Energy Models in Scalar-Tensor Theory of Gravitation” *East European Journal of Physics* 2 (2024): 48. http://dx.doi.org/10.26565/2312-4334-2024-2-04.

71.Luongo, O., Muccino, M. “Kinematic constraints beyond z≃0 using calibrated GRB correlations.” *A&A*, 641 (2020): A17. https://doi.org/10.1051/0004-6361/202038264

72.Luongo, O., Muccino, M. “Model-independent calibrations of gamma-ray bursts using machine learning.” *Monthly Notices of the Royal Astronomical Society*, 503(3) (2021): 4581. https://doi.org/10.1093/mnras/stab795

73.Luongo, O., Muccino, M. “Model independent cosmographic constraints from DESI 2024.” arXiv:2404.07070 (2024).

74.Carloni, Y., Luongo, O., & Muccino, M., “Does dark energy really revive using DESI 2024 data?.” arXiv:2404.12068 (2024)

75.Capozziello, S., Ruchika, & Sen, A. A. “Model-independent constraints on dark energy evolution from low-redshift observations.” *Monthly Notices of the Royal Astronomical Society*, 484(4) (2019): 4484-4494. doi: 10.1093/mnras/stz176.

76.Amirhashchi, H., Amirhashchi, S. “Current Constraints on Anisotropic and Isotropic Dark Energy Models.” *Phys. Rev. D* 99 (2019): 023516. doi:10.48550/arXiv.1803.08447

Information about authors:

G. Eswara Rao – M.Sc., Sri G.C.S.R. College, Rajam-532127, India, e-mail: eswararao.g@sgcsrc.edu.in

V. Ganesh – PhD, Assistant Professor, GIET University, Gunupur-765002, India, e-mail: vganesh@gmail.com

Y. Aditya – PhD, Assistant Professor, GMR Institute of Technology, Rajam-532127, India, e-mail: aditya.y@gmrit.edu.in; yaditya2@gmail.com

U.Y. Divya Prasanthi – PhD, Assistant Professor, Dr. Y.S.R. Horticultural University, Parvathipuram-535502, India, e-mail: divyaaug24@gmail.com